Unimolecular and Bimolecular Reactions of the .beta.-Distonic Ion CH3CH2OH+CH2CH2.bul.: An Experimental and Theoretical Study

ARTICLE *in* THE JOURNAL OF PHYSICAL CHEMISTRY · JULY 1995

Impact Factor: 2.78 · DOI: 10.1021/j100027a026

Unimolecular and Bimolecular Reactions of the β-Distonic Ion $CH_3CH_2OH^+CH_2CH_2^•$: An Experimental and Theoretical Study

Valérie Brenner,† Arielle Milliet, Philippe Mourgues, Gilles Ohanessian, and Henri-Edouard Audier*

Laboratoire des Mécanismes Réactionnels, URA 1307 du CNRS, Ecole Polytechnique, 91128 Palaiseau Cedex, France

Received: February 24, 1995; In Final Form: May 3, 1995[⊗]

In the gas phase, the unimolecular reaction of the metastable β-distonic ion **1**, $CH_3CH_2OH^+CH_2CH_2^•$, yields a CH_3CHOH^+ fragment ion. Experiments using isotopomers of **1** and ab initio calculations show that two pathways lead to its dissociation: (i) a 1,4-H migration leading to the α-distonic ion **2**, $CH_3CH^•OH^+CH_2$-CH_3, with subsequent elimination of $C_2H_5^•$; (ii) a H transfer within a $[C_2H_5OH, C_2H_4]^{•+}$ intermediate complex **3** followed by loss of $C_2H_5^•$. Two isomerization processes can occur prior to dissociation: a rapid permutation of the CH_2 groups in the radical chain and a reversible 1,5-H migration. The calculated transition state for 1,5-H migration and those arising on the fragmentation pathways are close in energy and correspond to relatively high energy barriers (93-100 kJ/mol), in agreement with the isotope effects observed. Finally, the bimolecular reactions of **1** with several neutral molecules are shown to be accompanied by the same 1,4- and 1,5-H migrations. The structures of the different isomeric ions thus formed were characterized by their specific ion−molecule reactions. The energy required for the various processes observed arises from the stabilization in the initial encounter complexes between **1** and each neutral molecule.

Introduction

A distonic cation is a radical cation which formally arises from ionization of a diradical or a zwitterion.[1-4] In such a structure (most often an isomer of a classical radical cation), charge and radical are borne by different atoms in a conventional valence bond description (Scheme 1).

In the gas phase, these species are key intermediates[3,4] in the unimolecular reactions of classical radical cations (Scheme 2) as well as in their bimolecular reactions.

A substantial body of experimental and theoretical work has shown that simple α-[5-7] and β-distonic ions[8-10] (Scheme 1) often correspond to energy minima on the potential energy surfaces (PESs) and that they are separated by substantial energy barriers from their conventional molecular ion counterparts. A variety of experimental techniques such as collisional activation (CA)[11,12] or neutralization−reionization mass spectrometry (NRMS)[13] enable the characterization of these ions, and specific bimolecular reactions[14] of α-[15-17] or β-distonic[18-21] ions occur.

The behavior of a β-distonic ion is rather complicated when several alkyl chains are present. In such a case the unimolecular dissociations or bimolecular reactions can be preceded by sequential H atom migrations from one chain to the other, leading to the isomerization of the initial ion[22-26] (Scheme 3).

These hydrogen migrations play a determining role, but the corresponding energy barriers have not yet been determined.

In this work, unimolecular reactions of the metastable $^•CH_2$-$CH_2OH^+CH_2CH_3$ β-distonic ion **1** were studied. In order to get further insight into the observed unimolecular isomerizations, the $C_4H_{10}O^{+•}$ PES was explored through high-level ab initio calculations. Moreover, for the first time, bimolecular reactions (performed in a Fourier transform ion cyclotron resonance (FT-ICR) spectrometer) have been used to characterize the structure

SCHEME 1

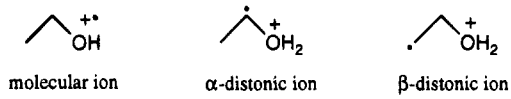

SCHEME 2

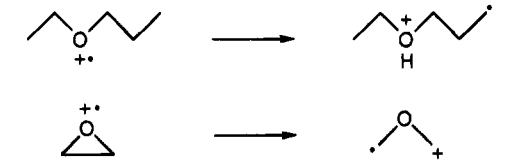

SCHEME 3

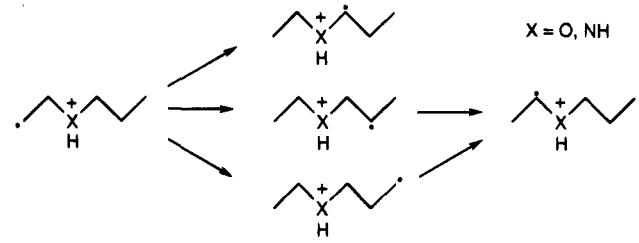

of each distonic ion resulting from the isomerization of the initially formed ion.

Experimental and Computational Section

Unimolecular Studies. Ion **1**, $^•CH_2CH_2OH^+CH_2CH_3$, and its labeled analogues were generated by fragmentation in the ion source of appropriately labeled and ionized 1-ethoxy-2-propoxyethane or 1,2-diethoxyethane (Scheme 4). These ethers were prepared by standard methods detailed elsewhere.[27] Recently, it has been shown[28] that the formation of labeled ions **1** is not preceded by any H/D exchange.

Unimolecular reactions close to threshold were studied by mass-analyzed ion kinetic energy (MIKE) spectrometry[29] in the

† Present address: Laboratoire de Chimie Théorique, DSM/DRECAM/SPAM, CE-CEA Saclay, 91191 Gif-sur-Yvette, France.

[⊗] Abstract published in *Advance ACS Abstracts*, June 1, 1995.

0022-3654/95/2099-10837$09.00/0

SCHEME 4

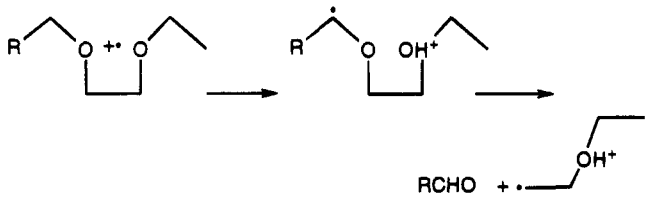

second field-free region (2nd FFR) of a double-focusing, reverse geometry VG ZAB-2F mass spectrometer, under standard operating conditions: ionizing electron energy 70 eV and accelerating potential 8 kV. Collisional activation (CA) reactions were examined after collision with helium; normally, the collision gas pressure was adjusted so as to reduce the intensity of the main beam signal by 50%. The kinetic energy releases (KERs) were determined after correction of the width of the main beam and calculated from the width at half-height (T_{50}). Metastable ion fragmentations in the first FFR were observed using linked B/E scans.[29]

Calculations. Ab initio molecular orbital calculations were carried out with the HONDO 8.1[30] and Gaussian 92 packages.[31] Optimized geometries have been obtained at the Hartree–Fock level (HF) with the 6-31G** basis set[32] (six-component d sets, leading to a total of 125 basis functions). Geometry optimization was carried out without any structural constraint. For the open-shell species, the spin-unrestricted Hartree–Fock (UHF) formalism was used and the energies were obtained after annihilation of unwanted spin states. The effects of electron correlation have been incorporated at the levels of second (MP2), third (MP3), and fourth (MP4) order Moller–Plesset perturbation theory. Calculations at all MP*n* levels (restricted to valence electrons) were performed with the 6-31G** basis set at the optimized HF/6-31G** geometries. As for the HF level, the energies of the open-shell species have been determined with the spin-unrestricted formalism (UMP*n*) after annihilation of unwanted spin states.

Vibrational frequencies were calculated at the HF level with the 6-31G** basis set in order to establish that optimized species were true minima (equilibrium structures) or saddle points (transition states) and to allow the evaluation of the zero-point vibrational energy (ZPVE). Since HF calculations are known to overestimate vibrational frequencies, the ZPVE have been obtained by scaling the calculated HF/6-31G** values by a factor of 0.89.[33] Finally, the highest level of computations can be summarized as MP4/6-31G**//HF/6-31G** + ZPVE.

Bimolecular Studies. Bimolecular reactions were studied with a Bruker CMS-47X FT-ICR spectrometer equipped with an external ion source. The β-distonic ions were produced from the same diether precursors as above. The neutral reactants were introduced through a leak valve (Balzers) at a pressure of 2×10^{-8} mbar and diluted in an argon bath (total pressure 1.5×10^{-7} mbar).

Isolation of the distonic ion, after transfer to the ICR cell, was performed by rf ejection of all unwanted ions. After a thermalization delay of 1 s, the parent ions were isolated again and allowed to react.

When necessary, high-resolution measurements were performed to check the isotopic composition of the product ions.

Energy-controlled CA spectra were recorded by exciting kinetically the ions (center of mass energy 60 eV) and letting them collide with argon (argon pressure 10^{-7} mbar, collision time 100 ms).

Results and Discussion

Unimolecular Reactions. The reaction of the β-distonic ion **1**, $^{\bullet}CH_2CH_2OH^+CH_2CH_3$, in the 2nd FFR is mainly dissociation

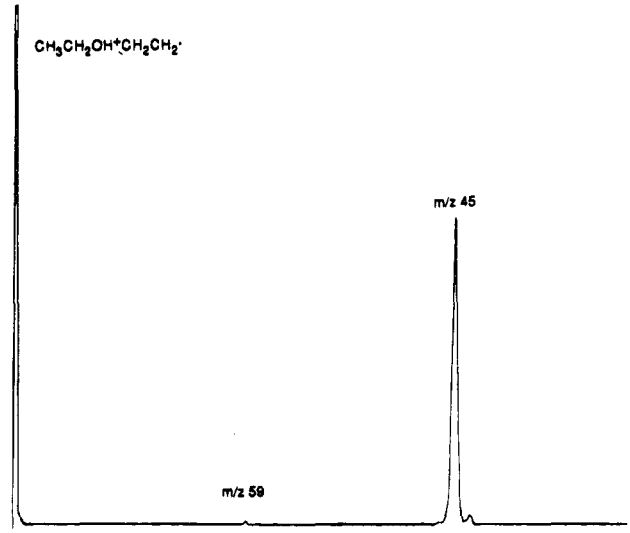

Figure 1. MIKE spectrum of **1**.

SCHEME 5

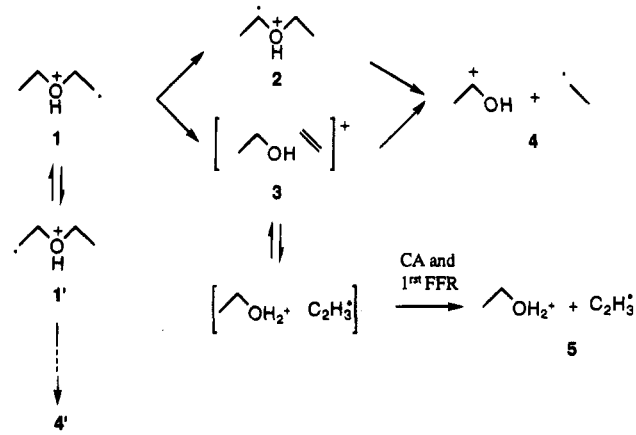

to a fragment ion at *m/z* 45 (96%) and also to a few fragment ions at *m/z* 44 (3%) and 59 (1%) (Figure 1). This behavior is completely different from that of diethyl ether radical cation (Table 1). A straightforward pathway to the *m/z* 45 fragment ion from **1** is a 1,4-H migration from a methylene group to the radical followed by the cleavage of the α-distonic ion **2** so formed. In another hypothesis, **1** fragments to form an ion–neutral $[CH_3CH_2OH, CH_2{=}CH_2]^{\bullet+}$ complex **3** in which H transfer from ethanol to ethylene leads to protonated ethanal by loss of an ethyl radical. Both processes give protonated ethanal (Scheme 5).

Formation of the *m/z* 45 fragment ion by simple cleavage of **1** can be a priori ruled out: such a process would involve protonated epoxide as an intermediate, which is much too high in energy (108 kJ/mol above protonated ethanal). Similarly, formation of the α-distonic ion **2** through a 1,2-H migration within the radical chain of **1** has been shown not to occur in other β-distonic ions[26] and therefore cannot be invoked in the mechanism leading to the formation of protonated ethanal.

In the 1st FFR (Table 2) or under collisional activation (Table 3), a new fragment ion appears at *m/z* 47, corresponding to protonated ethanol formation. For all fragmentations, carbon permutation and H exchanges take place prior to dissociation.

CH_2 Permutation in the Radical Chain. As for other β-distonic ions,[4,8,22,24,34] the similar behavior of **1f** and **1g** indicates that metastable (Tables 1 and 2) and stable (Table 3) ions **1** undergo a rapid permutation of both CH_2 groups of the radical chain. This permutation either results from a concerted

TABLE 1: MIKE Spectra of Labeled β-Distonic Ions 1

	m/z											
	44	45	46	47	48	49	59	60	61	62	63	73
$CH_3CH_2OH^+CH_2CH_2^\bullet$ (**1**)	3 (20)	96 (29)					1 (19)					
$CH_3CH_2OD^+CH_2CH_2^\bullet$ (**1a**)		8	91					1				
$CD_3CH_2OH^+CH_2CH_2^\bullet$ (**1b**)			6	1	92		1					
$CH_3CD_2OH^+CH_2CH_2^\bullet$ (**1c**)	1	40	51	7					1			
$CD_3CD_2OH^+CH_2CH_2^\bullet$ (**1d**)			8	3	1	87			1			
$CH_3CH_2OH^+CD_2CD_2^\bullet$ (**1e**)	3	70	4		22				<1		<1	
$CH_3CH_2OH^+CD_2CH_2^\bullet$ (**1f**)	2	73	9	14	2				<1			
$CH_3CH_2OH^+CH_2CD_2^\bullet$ (**1g**)	3	72	9	14	1				<1			
$CH_3{}^{13}CH_2OH^+CH_2CH_2^\bullet$ (**1h**)	1	27	71					<1				
$^{13}CH_3CH_2OH^+CH_2CH_2^\bullet$ (**1i**)	1	23	76					<1				
$CH_3CH_2OCH_2CH_3^{+\bullet}$ (**0**)		<1	<1			3						96

TABLE 2: B/E Linked Scan Fragmentations of Metastable Labeled Ions 1 in the 1st FFR

	m/z								
	44	45	46	47	48	49	50	51	52
$CH_3CH_2OH^+CH_2CH_2^\bullet$ (**1**)	2	93		5					
$CH_3CH_2OD^+CH_2CH_2^\bullet$ (**1a**)		16	80	2	2				
$CD_3CH_2OH^+CH_2CH_2^\bullet$ (**1b**)			5	1	90		4		
$CH_3CD_2OH^+CH_2CH_2^\bullet$ (**1c**)	1	28	66	3		2			
$CD_3CD_2OH^+CH_2CH_2^\bullet$ (**1d**)			7	2	1	89			1
$CH_3CH_2OH^+CD_2CD_2^\bullet$ (**1e**)	2	72	6		18	1	1		
$CH_3CH_2OH^+CD_2CH_2^\bullet$ (**1f**)	2	72	14	10	2				
$CH_3CH_2OH^+CH_2CD_2^\bullet$ (**1g**)	2	72	13	11	2				
$CH_3{}^{13}CH_2OH^+CH_2CH_2^\bullet$ (**1h**)	2	19	71	2	6				

process or involves the ion–neutral complex **3** as an intermediate (Scheme 6).

1,5-H Migration. In the MIKE spectrum of the ^{13}C-labeled ion **1h**, the protonated ethanal fragment ion *m/z* 45 is 71% shifted to *m/z* 46. Similarly, ion **1i** yields *m/z* 46 (76%) and *m/z* 45 (23%) fragment ions. Therefore, the protonated ethanal fragment ion contains mostly the initial ethyl chain carbon atoms and some radical chain carbon atoms. This result suggests that the dissociation can be preceded by a reversible 1,5-H migration (Scheme 7).[35] This **1** ↔ **1′** isomerization does not reach equilibrium as shown, for **1i**, by the abundance ratio (*m/z* 46)/(*m/z* 45) = 3.3. Most probably, the 1,5-H transfer competes with the 1,4-H migration leading to dissociation products.

This 1,5-H migration is accompanied by an important isotope effect, as shown by the small abundance of the *m/z* 46 fragment ions deriving from **1b** and **1d** (Scheme 7).[35] For **1b**, the intensity ratio of the directly formed protonated ethanal and the fragment ion resulting from a first 1,5-D migration is (*m/z* 48)/*m/z* 46) = 15.3, which must be compared with the ratio (*m/z* 46)(*m/z* 45) = 3.3 for **1i**. For this reason, the reversibility of **1** ↔ **1′** isomerization is hidden for deuterated compounds **1b** and **1d**. For instance for **1e** after a first 1,5-H migration, the isotope effect favors the return of the same hydrogen.

Intramolecular or Complex-Mediated 1,4-H Migration. Protonated ethanal formation may result from an intramolecular 1,4-H migration in the β-distonic ion **1** leading to an α-distonic ion **2** or from a hydrogen transfer within a transient ion–neutral complex **3** (Scheme 5). Whatever the process is, this H migration is subjected to a noticeable isotope effect, as shown

SCHEME 6

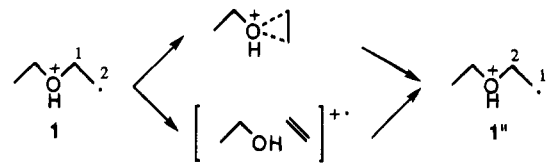

SCHEME 7

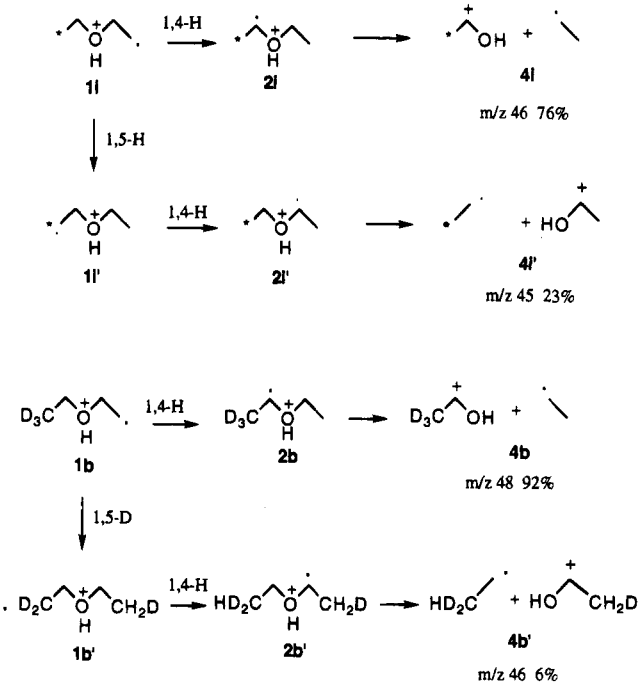

TABLE 3: CA Spectra of Labeled β-Distonic Ions 1

	m/z																				
	26	27	28	29	30	31	32	33	34	43	44	45	46	47	48	49	50	51	52	59	73
1	2	5.5	5.5	6.5		6				2.5	3	57.5	1.5	10							
1a	2.5	6.5	6.5	7	2	1	6			2	1	11	44	2.5	8						
1b	3	5.5	7	6.5	3	8	5			1.5	1	1.5	4	1	42	1	10				
1c	2	5	8	4	4	7	1	8		2	3	11	33	2	1	9					
1d	1	3	4.5	1	5	1	2	6	4	1	2	1	5	1.5		50.5		0.5	11		
1e	1	2	2.5	5	4.5	4.5	5.5	2		1	2	43	8	1.5	13	3	1	0.5			
1f	1.5	4	4	8	6	6				2	2	44	8	9	5	0.5					
1g	1.5	3	4	8	6	6				2	2	43	9	11	4	0.5					
1h		3	5	2	4	1	3			1	2	15	54	2	8						
1i	1	3	5	2	4	6				1	2	11	53	1	11						
0	2	5	2	11	1	16				2	1	8								43	9

SCHEME 8

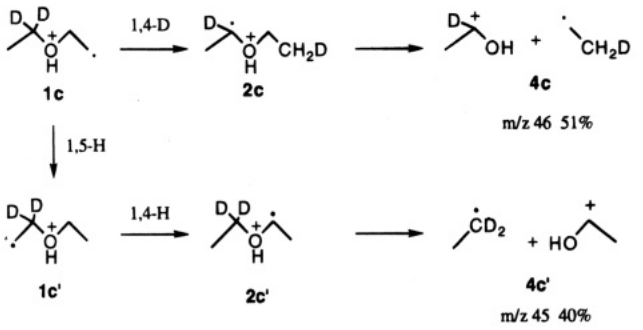

by the MIKE spectrum of **1c**. In **1c**, the direct formation of protonated ethanal (*m/z* 46) involves a D transfer, while *m/z* 45 formation only requires H transfers (Scheme 8).[35] In this case, the ratio (*m/z* 46)/(*m/z* 45) = 1.3 is smaller than the corresponding value for **1i**, in which H transfers are free from any isotope effects.

Two arguments suggest that, at least partly, the 1,4-H migration is complex-mediated. First, formation of protonated ethanol, *m/z* 47, in the 1st FFR as well as under CA argues in favor of this statement. Second the labeling indicates (**1a**, Table 1) that a small proportion of the initial ions undergo the exchange of the O-bonded hydrogen prior to dissociation. Since it has been shown (vide supra) that diethyl ether radical cation cannot be an intermediate in the fragmentation of **1**, neither 1,3-H shift from oxygen to radical carbon atom in **1** nor 1,2-H shift in **2** can occur in the field-free regions. Therefore, the exchange of the O-bonded hydrogen prior to protonated ethanol formation may be rationalized by an incomplete interconversion of $[C_2H_5OH, C_2H_4]^{\bullet+}$ and $[C_2H_5OH_2^+, C_2H_3^{\bullet}]$ ion−neutral complexes. Only the most energetic metastable ions **1** undergo this exchange, which is more important for the decompositions occurring in the 1st FFR.

The lack of protonated ethanol in MIKE spectra gives an estimate of the upper energy limit (789 kJ/mol) of the energy profile of the fragmentation of the decomposing ions in the 2nd FFR. This will be confirmed by ab initio calculations (vide infra).

Ab Initio Calculations. *Geometries.* Optimized HF/6-31G** geometries of the $[C_4,H_{10},O]^{\bullet+}$ ions are displayed in Figures 2−4. Bond lengths are given in angstroms and angles in degrees. The total energies at the different levels (HF//HF and MPn//HF) plus the ZPVE are given in Table 4. Moreover, for the open-shell species, we report in Table 4 the HF-calculated value of $\langle S^2 \rangle$ before annhilation of unwanted spin states.

We are unaware of any previous theoretical studies of ions **1** and **2**. The optimized structure of **1** has the methyl group staggered with respect to the adjacent CH_2 group and CCOC trans. The terminal CH_2 group is in the plane perpendicular to the plane defined by the adjacent C−C and C−O bonds. By contrast with $^{\bullet}CH_2CH_2OH_2^+$,[8,9] in which the C−O bond is significantly stretched, the C−O bond has a standard length in **1**. Ion **2** has the two terminal methyl groups staggered with respect to the adjacent C−O bond and CCOC trans. The CH group is staggered with respect to the OH group.

The structures of the various dissociation products in **4**, **6**, and **7** have already been described in the literature.[8,36,37] Particularly relevant is the structure of the ethanol radical cation previously obtained by Bouma et al.[8] at the HF/4-31G level. This ion resembles a complex between CH_2OH^+ and CH_3, with an elongated C−C bond of 1.999 Å, whereas the C−O and the methyl C−H bonds are short: 1.281 and 1.077 Å, respectively.

The results of the ab initio calculations for **5** (protonated ethanol plus vinyl radical) are not reported here. This is due

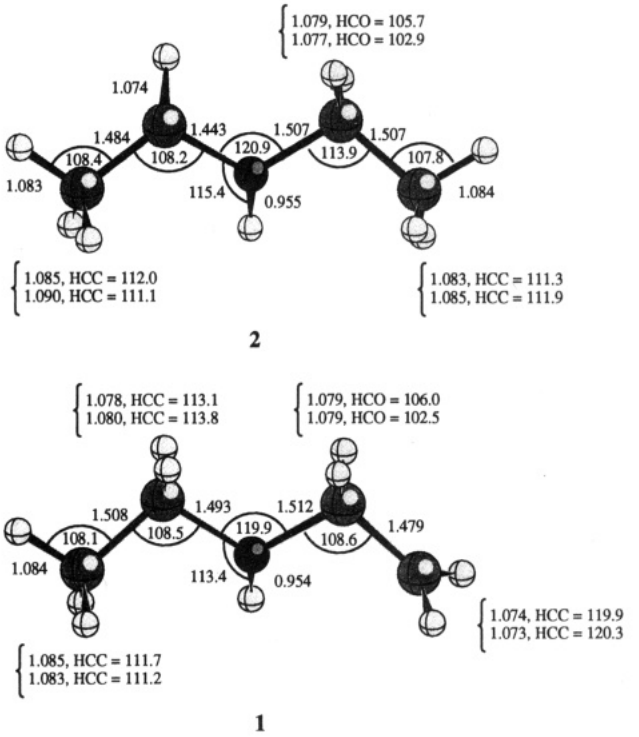

Figure 2. Optimized HF/6-31G** geometries of **1** and **2**. The distances are in angstroms and the angles in degrees.

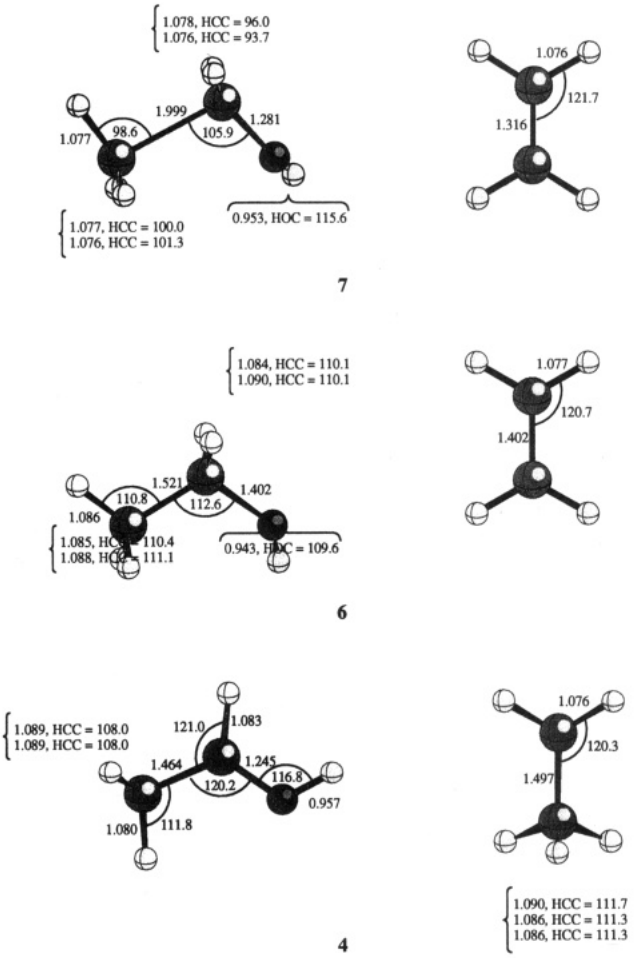

Figure 3. Optimized HF/6-31G** geometries of the dissociation products **4**, **6**, and **7**. The distances are in angstroms and the angles in degrees.

to the important discrepancy between the HF-calculated $\langle S^2 \rangle$ value, 1.014, of the vinyl radical (σ radical) and the true value

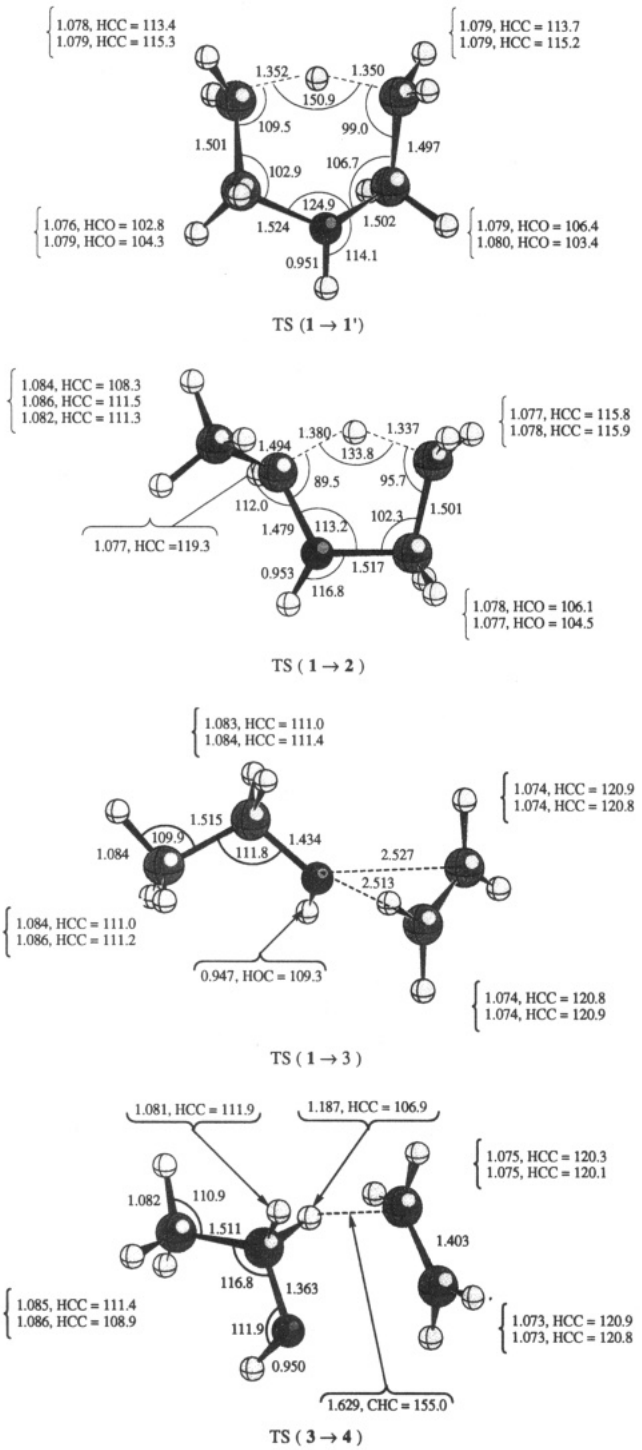

Figure 4. Optimized HF/6-31G** geometries of the transition states TS(**1**→**1'**), TS(**1**→**2**), TS(**1**→**3**), and TS(**3**→**4**). The distances are in angstroms and the angles in degrees.

of a pure doublet, which is 0.75. In this way, the energies obtained after annhilation of unwanted spin states (the wave function is truncated) do not give a reasonable approximation of the true values (optimization of the wave function), and it seems more appropriate to use the experimental data for **5** to position its energy. On the contrary, the other fragmentation products and the equilibrium structures have values of $\langle S^2 \rangle$ which vary from 0.754 to 0.768, whereas the values for the transition states are between 0.755 and 0.793. Therefore, the energies obtained after annihilation of unwanted spin states probably yield an accurate approximation of the true energy for the other fragmentation products and the equilibrium structures, and nearly so for the transition states.

It is important to note that the geometry optimization of the ion−neutral complex **3** between ethanol and the ethylene radical cation could not be performed completely in spite of an important exploration of the relevant portion of the PES. This can be explained by the fact that this portion of the PES, connected to the transition state TS(**1** → **3**), which has been well characterized (see below), is very flat. Indeed, for variations of the interfragment distances up to ±0.3 Å, the total energy values differ only by ±0.1 kJ/mol. We did not succeed in eliminating all imaginary frequencies in this case. Consequently, we do not present the results for this ion in figures or in tables; however, we will see below that this does not prevent comparison with experiments.

The transition states TS (**1** → **1'**) and TS(**1** → **2**) correspond to cyclic structures. In TS (**1** → **1'**), the ethyl and the CH_2-$CH_2^\bullet$ groups are twisted by about 180° with respect to their positions in ion **1**, whereas in TS(**1** → **2**), only the $CH_2CH_2^\bullet$ group is twisted. The distances between the migrating hydrogen and the two carbon atoms involved in the migration are equivalent in TS(**1** → **1'**): 1.352 vs 1.350 Å. In TS(**1** → **2**), these distances differ and the distance between the migrating hydrogen and the initial carbon atom is somewhat larger: 1.380 vs 1.337 Å. The angle between the three atoms involved in the migration is larger in TS(**1** → **1'**) than in TS(**1** → **2**): 150.9° as compared to 133.8°. The cyclic structure determined for TS-(**1** → **2**) is similar to that optimized at the same level of calculation by McAdoo et al.[26] for $CH_3OH^+CH_2CH_2^\bullet$, where the distances between the migrating hydrogen and the two carbon atoms are equal to 1.390 and 1.323 Å and the angle made by these three atoms is 132.9°. The transition state TS(**1** → **3**) corresponds to a structure where the $CH_2CH_2^\bullet$ group is in a plane perpendicular to that formed by the heavy atoms of the ethanol. One of the carbon atoms is slightly closer to the oxygen atom: 2.513 vs 2.527 Å. The analysis of the mode associated with the imaginary frequency of this transition state shows that it is connected on one side to **1** and on the other side to a very flat portion of the PES which corresponds to **3**, the ion−neutral complex. Consequently, in spite of the noncharacterization of **3**, it is well established that the transition state TS(**1** → **3**) does not correspond to a rotation of the CH_2CH_2 group but to a O−C bond cleavage leading to the formation of the ion−neutral complex. It is difficult to decide whether isomerization of **1** to **1''** corresponds to a specific transition state or if it involves first TS(**1** → **3**), formation of **3**, and then formation of **1''** through a second TS analogous to TS(**1** → **3**). In any case, the potential energy surface is very flat in this region, and the energy of TS(**1** → **3**) should give a good approximation to that of TS-(**1** → **1''**), whatever exact structure it has. In the transition state TS(**3** → **4**), one C−H bond of the CH_2 group of the ethanol is elongated (1.187 Å) and the hydrogen atom points toward one of the carbon atoms of the CH_2CH_2 moiety with a C−H distance of 1.629 Å.

Energies. In order to analyze these results in more detail, we report in Table 5, for each level of theory and taking **1** as the reference, the relative energies of the $[C_4,H_{10},O]^{\bullet+}$ systems with the ZPVE correction. Moreover, in order to test the reliability of the calculations and assess the uncertainties in our relative energy values, the available experimental enthalpies of formation at 0 K[38] are included in Table 5.

The most stable system at all levels of calculation is **1**, the β-distonic ion. The order of stability of the various structures is unchanged from the HF to the MP4 level. However, depending on the level of theory applied, the effects of electron correlation on the energies of the various species relative to that of **1** are different. The relative energy of **2** is insensitive

TABLE 4: Total Energies of $[C_4, H_{10}, O]^{\bullet+}$ Ions

ion	S^2 [a]	HF/6-31G**[b]	ZPVE[c]	MP2/6-31G**// HF/6-31G**[b]	MP3/6-31G**// HF/6-31G**[b]	MP4/6-31G**// HF/6-31G**[b]
$CH_3CH_2OH^+CH_2CH_2^\bullet$ (**1**)	0.761	−231.865 507	381.1	−232.589 412	−232.640 288	−232.670 176
$CH_3CH^\bullet OH^+CH_2CH_3$ (**2**)	0.760	−231.860 504	378.9	−232.584 541	−232.635 307	−232.665 102
$CH_3CH^+OH + CH_3CH_2^\bullet$ (**4**)	0; 0.762	−231.848 986	360.2	−232.562 032	−232.613 104	−232.644 331
$CH_3CH_2OH + CH_2CH_2^{\bullet+}$ (**6**)	0; 0.754	−231.810 797	365.7	−232.515 651	−232.571 643	−232.597 974
$CH_3CH_2OH^{\bullet+} + CH_2CH_2$ (**7**)	0.768; 0	−231.789 850	362.5	−232.512 267	−232.563 179	−232.596 452
TS (**1** → **1′**)[d]	0.791	−231.811 449	368.9	−232.548 185	−232.595 464	−232.628 068
TS (**1** → **2**)	0.794	−231.809 748	369.2	−232.548 695	−232.595 503	−232.628 536
TS (**1** → **3**)	0.755	−231.839 873	369.9	−232.555 414	−232.609 000	−232.638 521
TS (**3** → **4**)	0.772	−231.818 004	367.1	−232.547 109	−232.597 306	−232.630 296

[a] Mean value of S^2 for the radicals at the HF level. [b] SCF (MP*n*) energies (hartrees) are obtained by a RHF (RMP*n*) calculation for the closed-shell species and UHF (UMP*n*) calculation after annihilation of unwanted spin states for open-shell species. [c] Values (kJ/mol) are from frequencies at the HF/6-31G** level. [d] This transition state corresponds to the intramolecular 1,5-H migration. Ion **1′** is $^\bullet CH_2CH_2OH^+CH_2CH_3$.

TABLE 5: Relative ab Initio Energies of $[C_4, H_{10}, O]^{\bullet+}$ Ions

ion	$\Delta E_{HF/6\text{-}31G^{**}}$[a] with ZPVE	$\Delta E_{MP2/6\text{-}31G^{**}//HF/6\text{-}31G^{**}}$[a] with ZPVE	$\Delta E_{MP3/6\text{-}31G^{**}//HF/6\text{-}31G^{**}}$[a] with ZPVE	$\Delta E_{MP4/6\text{-}31G^{**}//HF/6\text{-}31G^{**}}$[a] with ZPVE	exptl[b]
$CH_3CH_2OH^+CH_2CH_2^\bullet$ (**1**)	0	0	0	0	
$CH_3CH^\bullet OH^+CH_2CH_3$ (**2**)	11	11	11	11	
$CH_3CH^+OH + CH_3CH_2^\bullet$ (**4**)	22	53	52	49	*724*[d]
$CH_3CH_2OH + CH_2CH_2^{\bullet+}$ (**6**)	129	180	166	176	857
$CH_3CH_2OH^{\bullet+} + CH_2CH_2$ (**7**)	180	186	185	177	854
TS(**1** → **1′**)[c]	130	97	107	100	
TS(**1** → **2**)	134	96	107	98	
TS(**1** → **3**)	56	79	72	73	
TS(**3** → **4**)	111	99	101	93	

[a] The ZPVE (zero-point vibrational energies) values (kJ/mol) are from frequencies at the HF/6-31G** level. For the MP*n* levels, these values are scaled by a factor of 0.89. [b] Experimental formation enthalpies at 0 K (kJ/mol) are from ref 38. [c] This transition state corresponds to the intramolecular 1,5-H migration. Ion **1′** is $^\bullet CH_2CH_2OH^+CH_2CH_3$. [d] Estimated value (see text).

to electron correlation. Those of the dissociation products **4**, **6** and **7** are larger at the MP2 than at the HF level, but this effect is reduced at higher levels. The relative energies of transition states for hydrogen migrations, TS(**1** → **1′**), TS(**1** → **2**), and TS(**3** → **4**), are smaller at the correlated than at the HF level, as expected for structures involving stretched bonds, with a nonmonotonic effect of perturbation order. Correlation effects are different for TS(**1** → **3**), possibly because it is very similar to an ion−neutral complex type of structure. In this case, the MP2 contribution raises the relative energy, but the effect is reduced at higher perturbation orders.

As expected, the value of the HF ZPVE correction varies with the type of structure: about 380 kJ/mol for the equilibrium structures, about 369 kJ/mol for the transition states, and about 363 kJ/mol for the dissociation products (see Table 4). Thus, the effect of ZPVE is to lower the relative energies of all transition states and dissociation products.

Energy Profile and Reaction Mechanism. The energy profile for the unimolecular reaction of **1**, based on the results at the MP4/6-31G**//HF/6-31G** level with ZPVE correction, is displayed in Figure 5, with **1** taken as the energy reference. Here, the relative energy of **5** is an average of the values obtained by combining the theoretical values obtained for **6** and **7** and the difference between the experimental enthalpies of formation at 0 K of **6**, **7** and **5**. As the experimental enthalpy of formation at 0 K of one species in **5**, protonated ethanol, is not available, it has been estimated from the value at 298 K and the difference between the values at 0 and 298 K of a similar species: ethanol. In this way, the formation enthalpy at 0 K of **5** is 787 kJ/mol, and thus the relative energy of **5** is 108 kJ/mol. With the same procedure, the formation enthalpy at 0 K of one species of **4**, protonated ethanal, can be estimated from the difference between the values at 0 and 298 K of ethanal. The enthalpy of formation at 0 K of **4** is then 724 kJ/mol, as compared to 730 and 726 kJ/mol, the values deduced from the theoretical values of **4**, **6**, and **7** and the experimental values of

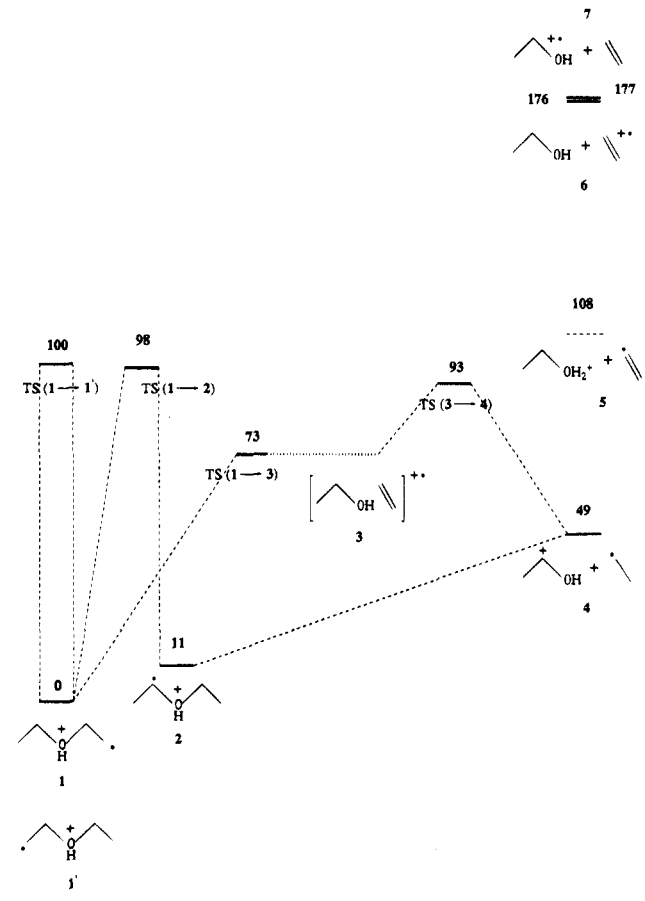

Figure 5. Computed energy profile (MP4/6-31G**//HF/6-31G** plus scaled HF ZPVE corrections) for the unimolecular reactions of CH_3-$CH_2OH^+CH_2CH_2^\bullet$.

6 and **7**. These values are in the range of uncertainties estimated for the calculations.

The β-distonic ion **1** is more stable than the α-distonic ion **2** by 11 kJ/mol. The ion−neutral complex **3** corresponds to a very flat portion of the PES, and the barrier to reach it from **1** (TS(**1** → **3**)) is the lowest of all: 73 kJ/mol. The H transfer in the ion−neutral complex which involves the transition state TS-(**3** → **4**) can occur with a barrier of 93 kJ/mol.

The isomerizations (**1** → **1'**) and (**1** → **2**), which correspond to the intramolecular 1,5- and 1,4-H migrations, respectively, involve high and similar barriers: the energies of the associated transition states differ by only 2 kJ/mol and the most stable transition state lies 98 kJ/mol above **1**. In a similar system, $CH_3OH^+CH_2CH_2^\bullet$, McAdoo et al.[26] have obtained, at the UMP2/6-31G** level, a barrier for the intramolecular 1,4-H transfer similar to ours: 117 kJ/mol.

These results are fully consistent with the experimentally observed reactions, as discussed below:

(1) The observed dissociation products **4** lie 49 kJ/mol higher than **1**. All of the transition states studied lie above **4** and below **5**, in agreement with the absence of protonated ethanol (*m/z* 47) in the MIKE spectrum of **1**. However, all are calculated to be close to **5**, implying that metastable ions decomposing in the 2nd FFR lie in a narrow range of internal energy. This is borne out by the presence of a small *m/z* 47 peak in the B/E linked scan spectrum of **1**, in which the decomposition of slightly more energetic ions can be observed. The relative intensity of the *m/z* 47 peak is even enhanced in the CA spectrum, as expected.

(2) The fact that the energy barriers for 1,5- and 1,4-H migrations are close to the maximum internal energy available is also consistent with the experimental observation of kinetic isotope effects for both processes.

(3) Finally, the calculations indicate that both 1,4-H migration followed by fragmentation (**1** → **2** → **4**) and formation of an ion−neutral complex in which H-transfer occurs before dissociation (**1** → **3** → **4**) are viable mechanisms for the formation of protonated ethanal since the highest energy barriers are 98 and 93 kJ/mol, respectively.

Bimolecular Reactions of Ion 1. Another way to characterize the particular structure of distonic ions is to study their bimolecular reactions.[4,14] The interest of such a study for ion **1** is to check whether it would reflect the unimolecular behavior and particularly if complexation energy with the neutral target could induce similar hydrogen transfers.

Evidence for 1,4-H Migrations. We have examined the bimolecular reactivity of ion **1** with a variety of neutral molecules, including acetone, acetonitrile, and dimethyl ether. Four reaction pathways are observed, namely, (1) proton transfer leading to the protonated neutral; (2) $C_2H_5O^+$ transfer (loss of $C_2H_5^\bullet$ from the encounter complex); (3) $C_2H_4^{+\bullet}$ transfer to the neutral target (loss of ethanol from the ion−molecule complex); (4) hydrogen abstraction from the neutral reactant, forming protonated diethyl ether. This reaction is not observed with acetonitrile.

In order to characterize the isomerization of the β-distonic ion **1** into the α-distonic ion **2**, the bimolecular reactions of **2** were studied. It is not possible to generate **2** directly in the ion source. However, it has been recently proved that, in bimolecular reactions of molecular ions, the formation of the products is often preceded by the catalyzed isomerization of the molecular ion into its α-distonic isomer.[16] More specifically, it has been shown[17] that the first step of the reaction of $C_2H_5OC_2H_5^{\bullet+}$ with a neutral molecule N is its isomerization to **2** within a complex. Only two reactions pathways are observed (Scheme 9), namely, (1) proton transfer leading to the protonated neutral and (2) $C_2H_5O^+$ transfer (loss of $C_2H_5^\bullet$ from the encounter complex).

SCHEME 9

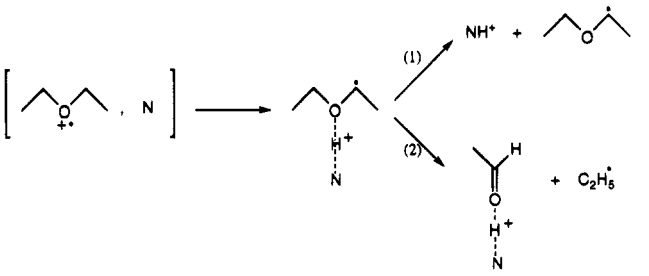

SCHEME 10

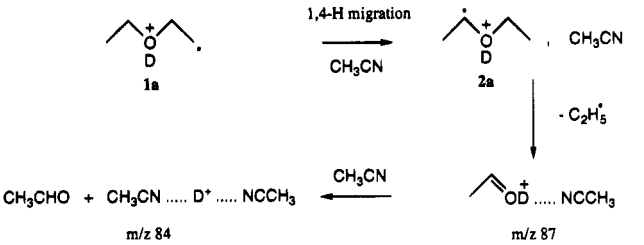

For **1**, as well as for ionized diethyl ether, the loss of $C_2H_5^\bullet$ (reaction 2) yields product ions which were proved to be proton-bound dimers with ethanal. Particularly, as the reaction time increases, these ions undergo a substitution of ethanal by the neutral molecule.

For instance, ion **1** reacts with hexadeuterated acetone to give a *m/z* 109 product ion $[(CD_3)_2CO{-}H^+{-}OCHCH_3]$, which in turn leads to the H^+-bound dimer of the neutral reactant (*m/z* 129), in agreement with the relative proton affinities. The relation was clearly established by continuous ejection at *m/z* 109 throughout the reaction time: this strongly diminishes the formation of *m/z* 129 ions.

Starting from **1**, the simplest process accounting for such a result is an isomerization of **1** into **2**, which then reacts as depicted in Scheme 9. This isomerization can be achieved by a simple 1,4-H migration.

The reaction of O-deuterated ion **1a** with acetonitrile also supports strongly a 1,4-H migration followed by the loss of $C_2H_5^\bullet$. An ion $C_4H_7DNO^+$, *m/z* 87, is obtained, and the further reaction of this ion gives the D^+-bound dimer *m/z* 84 of acetonitrile, retaining the deuterium atom (Scheme 10, Figure 6).

It is noteworthy that this 1,4 migration is subjected to a H/D isotope effect, which for instance prevents reaction 2 from occurring with acetone starting from the pentadeuterated ion **1d**.

Therefore, part of the bimolecular reactivity of **1**, namely, protonation of the neutral (reaction 1) and $C_2H_5^\bullet$ loss from the encounter complex (reaction 2), can be explained by an isomerization into **2** through a 1,4-H migration. By contrast, the initial β-distonic structure **1** is the reactive form for $C_2H_4^{\bullet+}$ transfer (reaction 3) and for the $H^\bullet$ abstraction process (reaction 4).

Finally, the lack of $C_2H_4^{\bullet+}$ transfer to the neutral (reaction 3) in the reactions of ionized diethyl ether proves that **2** formed by isomerization of this molecular ion does not isomerize into **1**. Otherwise stated, the reaction **1** → **2** is not reversible.

Evidence for 1,5-H Migrations. The reactivity of isotopically labeled ions **1** (Table 6) shows that both side chains of **1** contribute to transfer reactions 2 and 4, revealing hydrogen migrations which are similar to those observed in the unimolecular decompositions.

The transfer on the neutral reagent of an ethylene radical cation $C_2H_4^{\bullet+}$ is clearly characteristic of **1**, as has been described

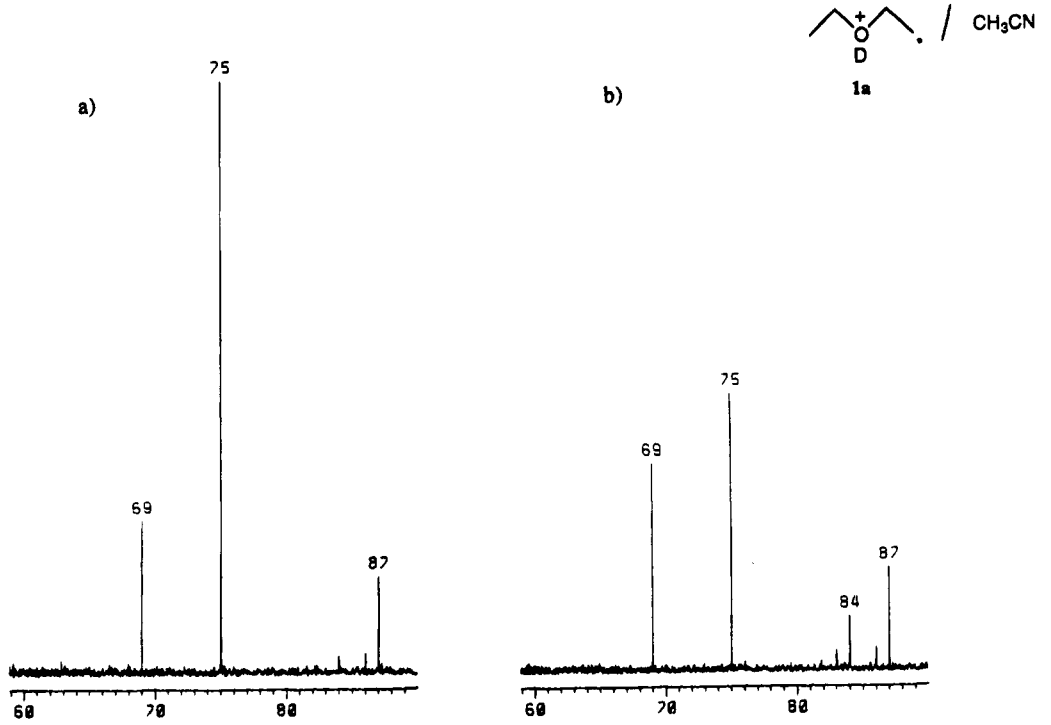

Figure 6. Reaction of **1a** with acetonitrile (1.5×10^{-8} mbar), partial spectra. Reaction time: (a) 4 s and (b) 8 s.

TABLE 6: Reactions of β-Distonic Ion 1 and Ionized Diethyl Ether with Acetonitrile, Acetone, and Dimethyl Ether

ion	neutral[a]	H^+ transfer		D• abstraction		$C_2H_4^{+\bullet}$ transfer		$C_2H_5O^+$ transfer[b]	
$C_2H_5OH^+CH_2CH_2^\bullet$	CD_3CN	*m/z* 45	100[c]			*m/z* 72	35	*m/z* 89	20
	CD_3COCD_3	*m/z* 65	40	*m/z* 76	100	*m/z* 92	50	*m/z* 109	25
	CD_3OCD_3	*m/z* 53	100	*m/z* 76	10	*m/z* 80	15	*m/z* 97	60
$C_2H_5OC_2H_5^{\bullet+}$	CD_3CN	*m/z* 45	20					*m/z* 89	100
	CD_3COCD_3	*m/z* 65	100					*m/z* 109	45
	CD_3OCD_3	*m/z* 53	30					*m/z* 97	100

[a] The fully deuterated neutral reactant was used to distinguish proton transfer from charge transfer followed by self-protonation. [b] At long reaction times, this ratio is lowered by further substitution of C_2H_4O by a neutral molecule (see text). [c] The origin of this high-level protonation is not clear. It was found that the O-bonded proton contributes only partially to this process.

TABLE 7: Transfers of Ionized Ethylene and Protonated Acetaldehyde in Bimolecular Reactions of Labeled Ions 1

labeled ion **1**	neutral	ionized ethylene transferred (*m/z* of product ions)			protonated acetaldehyde transferred[a] (*m/z* of product ions)		
$CH_3CH_2OD^+CH_2CH_2^\bullet$ (**1a**)	CH_3CN	**$C_2H_4^{\bullet+}$ only** (*m/z* 69)			**$C_2H_4OD^+$ only** (*m/z* 87)		
$CD_3CD_2OH^+CH_2CH_2^\bullet$ (**1d**)		**$C_2H_4^{\bullet+}$**	**$C_2H_3D^{\bullet+}$**	**$C_2D_4^{\bullet+}$**		**$C_2H_3DOH^+$**	**$C_2D_4OH^+$**
	CH_3CN	81 (*m/z* 69)	11 (*m/z* 70)	8 (*m/z* 73)		49 (*m/z* 87)	51 (*m/z* 90)
	CH_3COCH_3	100 (*m/z* 86)				not measurable	
$CH_3CH_2OH^+CD_2CD_2^\bullet$ (**1e**)		**$C_2H_4^{\bullet+}$**		**$C_2D_4^{\bullet+}$**	**$C_2H_4OH^+$**	**$C_2H_3DOH^+$**	**$C_2D_3HOH^+$**
	CD_3OCD_3	64 (*m/z* 80)		36 (*m/z* 84)	60 (*m/z* 97)	15 (*m/z* 98)	25 (*m/z* 100)
	CH_3CN	70 (*m/z* 69)		30 (*m/z* 73)	50 (*m/z* 86)	15 (*m/z* 87)	26 (*m/z* 89)[b]
							$C_2D_3HOD^+$
	CH_3COCH_3	57 (*m/z* 86)		43 (*m/z* 90)	63 (*m/z* 103)		37 (*m/z* 107)
$^{13}CH_3CH_2OH^+CH_2CH_2^\bullet$ (**1i**)		**$C_2H_4^{\bullet+}$**		**$^{13}CH_2CH_2^{\bullet+}$**	**$C_2H_4OH^+$**		**$^{13}CH_3CHOH^+$**
	CD_3OCD_3	65 (*m/z* 80)		35 (*m/z* 81)	43 (*m/z* 97)		57 (*m/z* 98)
	CD_3CN	65 (*m/z* 72)		35 (*m/z* 73)	44 (*m/z* 89)		56 (*m/z* 90)
	CH_3COCH_3	60 (*m/z* 86)		40 (*m/z* 87)	45 (*m/z* 103)		55 (*m/z* 104)

[a] At long reaction time, these product ions react further by substitution of acetaldehyde by the neutral molecules with retention of the H (or D) shown to be bound with oxygen. [b] Also transferred $C_2D_4HO^+$ (9%) along with some mono- and trideuterated ethylenes (less than 10%).

for analogous β-distonic ions.[18-21] In the cases so far published, it has been shown that it is the $^\bullet CH_2CH_2$ part of the ion which is transferred. However, the study of isotopically labeled ions **1** shows that both sides of the ion are involved in the $C_2H_4^{\bullet+}$ transfer. For instance, $^{13}CH_3CH_2OH^+CH_2CH_2^\bullet$, **1i**, transfers $C_2H_4^{\bullet+}$ and $^{13}CH_2CH_2^{\bullet+}$ in a 2:1 ratio on acetonitrile and dimethyl ether and in a 3:2 ratio on acetone (Table 7). This result provides direct evidence that a 1,5-H migration has occurred to a large extent, affording from **1** the symmetrical ion **1'**. Nevertheless, $C_2H_4^{\bullet+}$ transfer occurs predominantly from the initial structure of the distonic ion, at least when the reaction is free from any isotope effect.

As for unimolecular reactions, this 1,5-H migration is affected by a very strong H/D isotope effect: the pentadeuterated ion **1d** transfers exclusively $C_2H_4^{\bullet+}$ to acetone, and a minor proportion of $C_2D_4^{\bullet+}$ to acetonitrile.

The 1,5-H migration can be, in turn, followed by a 1,4-H migration. For instance, $^{13}CH_3CH_2OH^+CH_2CH_2^\bullet$, **1i**, yields, via

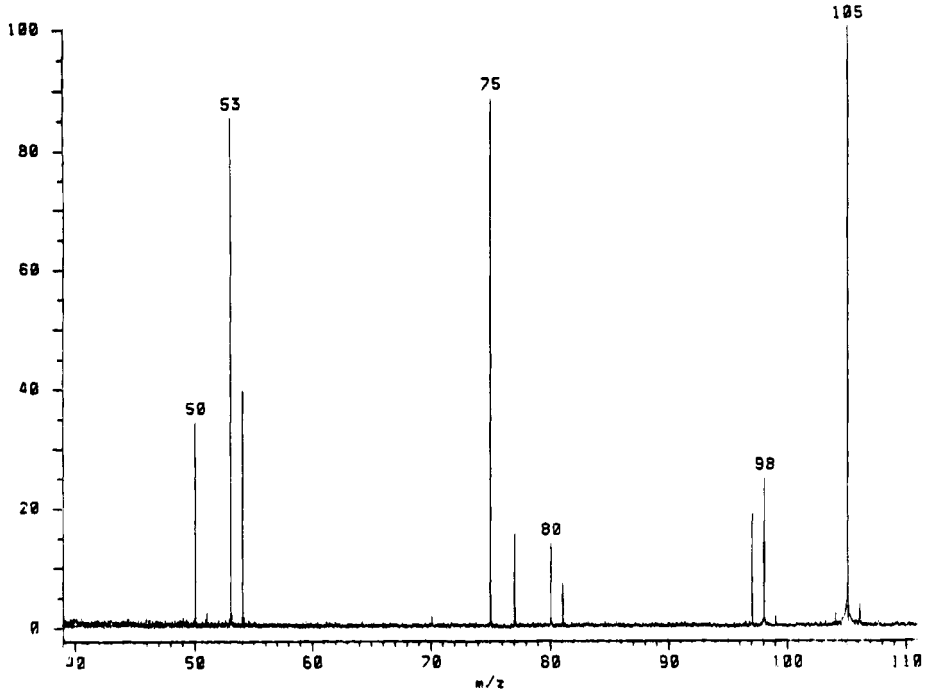

Figure 7. Reaction of $^{13}CH_3CH_2OH^+CH_2CH_2^\bullet$ (**1i**) with CD_3OCD_3 (pressure 3×10^{-8} mbar, reaction time 8s).

SCHEME 11

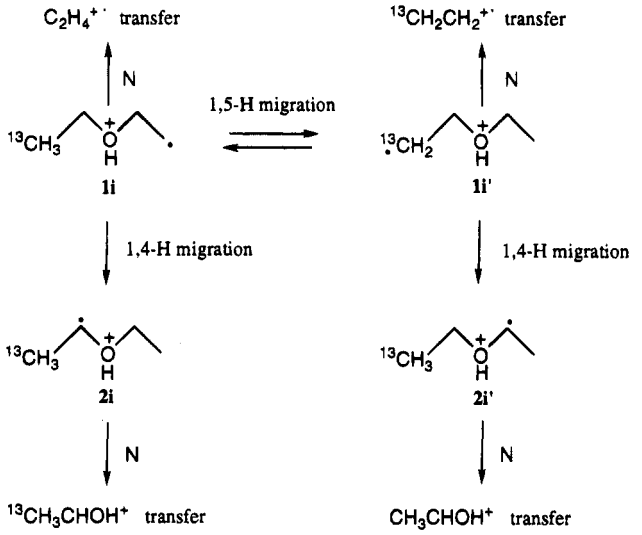

reaction 2, a mixture of $[CH_3CHO\cdots H^+\cdots N]$ and $[^{13}CH_3CHO\cdots H^+\cdots N]$ product ions. All the results show, therefore, that **1i** isomerizes into several reactive structures, namely, **1i'**, **2i**, and **2i'** (Scheme 11, Figure 7) prior to the reactions observed.

Reversibility of 1,5-H Migration. We just have seen that the ^{13}C-labeled ion **1i** reacts bimolecularly by transferring more $C_2H_4^{\bullet+}$ than $^{13}CH_2CH_2^{\bullet+}$. Reasonably assuming that there is no significant isotope effect in this case, this rules out a complete equilibration, by successive 1,5-H migrations, between **1** and **1'** prior to the transfer of ionized ethylene.

However, a partial reversibility of the 1,5-H migration cannot be discarded, and a careful analysis of the results shows that it is indeed the case.

For instance, the reaction of pentadeuterated ion **1d** with acetonitrile, besides the small transfer of $C_2D_4^{\bullet+}$ resulting from a 1,5-D migration (ions of *m/z* 73, see above), gives rise also to a significant signal at *m/z* 70. High-resolution measurement shows that it corresponds to a transfer of $C_2H_3D^{\bullet+}$ to CH_3CN and therefore to a double 1,5 migration prior to transfer.

SCHEME 12

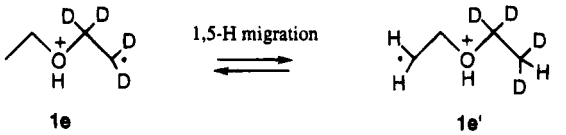

Such a reversibility could also explain the reactions of the tetradeuterated ion **1e** (Table 7), which transfers more $C_2H_4^{\bullet+}$ (from the structure **1e'**) than $C_2D_4^{\bullet+}$ (from the original one, **1e**). In this case, the strong H/D primary isotope effect affecting the 1,5 migration would reduce the efficiency of the back-migration, almost limited in this case to the H being originally shifted, and therefore enhance the weight of the **1e'** structure in the reactions (Scheme 12).[39]

Occurrence of Hydrogen Migrations during Ion–Molecule Reactions. It is important to know whether the H migrations described above occur during the ion–molecule reaction or if the thermalized ions isolated in the cell are already a mixture of distonic isomers. It is actually possible that hydrogen migrations occur in the external source where the ions are formed or during their flight toward the cell. They can also isomerize under collision with argon during the thermalization process.

Energy-controlled CA spectra were first recorded for the various labeled ions **1**, and among the fragments ionized ethylene is observed, originating from both side chains. This fragment ion is most probably formed by direct cleavage of the β-distonic ion's radical chain, so it could be thought to characterize the two structures **1** and **1'**. Unfortunately, the CA process is not free from hydrogen migrations and could not be used directly as a probe for the structure of the parent ions.

However, we can consider that, for instance, the 1:4 ratio observed for $^{13}CH_2CH_2^{\bullet+}/C_2H_4^{\bullet+}$ fragment ions in the CA spectrum of **1i** will correspond to an upper value of the proportion **1i'/1i** existing before the bimolecular reaction.

By contrast, ion **1i** transfers $^{13}CH_2CH_2^{\bullet+}$ and $C_2H_4^{\bullet+}$ to acetone in a 2:3 ratio. This demonstrates clearly that the 1,5-H migrations also occur during ion–molecule reactions.

The same question could be asked for 1,4-H migrations. For thermodynamic reasons (Figure 5), it is unlikely that such

migrations can lead to stable α-distonic ions **2**, as they would possess enough energy to decompose immediately. Therefore, the 1,4 migrations have to occur during the ion−molecule reaction.

The reactions of the β-distonic ion **1** during interaction with a neutral present an analogy with its unimolecular reactions worth noting. The same hydrogen migrations occur, and moreover, primary H/D isotope effects are observed in both cases. Therefore, analogous barriers for 1,4- and 1,5-H migrations may well exist in the bimolecular case also, although not necessarily of the same values.

Ion−neutral reactions are performed starting from thermally relaxed parent ions, which do not possess on their own enough energy to overcome such barriers. The desired energy has to come from the stabilizing interaction between the ion and the neutral target, and it would be interesting to know how much energy is available by this process.

Conclusions

The results presented in this paper lead to the following conclusions:

1. The β-distonic ion **1** corresponds to a deep well on the PES. In contrast to $^{\bullet}CH_2CH_2OH_2^+$,[8,9] in which the C−O bond is significantly stretched, the C−O bond has a standard length in **1**.

2. The spontaneous unimolecular dissociation of metastable ion **1** is preceded by H migrations. These migrations require high energy barriers and are rate-determining. The intermediacy of an ion−neutral complex in the fragmentation leading to protonated ethanal is highly probable. However, calculations show that this fragment can also be formed via a direct 1,4-H migration. The transition state for 1,5-H migration and those for fragmentation are very close in energy. This is in agreement with the substantial isotope effects observed.

3. The bimolecular reactions of **1** present a noteworthy analogy with its unimolecular decomposition. In both cases, the same hydrogen migrations occur, and primary H/D isotope effects are observed, suggesting analogous energy barriers.

References and Notes

(1) Yates, B. F.; Bouma, W. J.; Radom, L. *J. Am. Chem. Soc.* **1984**, *106*, 5805.

(2) Radom, L.; Bouma, W. J.; Nobes, R. H.; Yates, B. F. *Pure Appl. Chem.* **1984**, *56*, 1831.

(3) (a) Schwarz, H. *Nachr. Chem., Tech. Lab.* **1983**, *31*, 451. (b) Schwarz, H. *Shitsuryo Bunseki* **1984**, *32*, 3.

(4) For a review, see: Hammerum, S. *Mass Spectrom. Rev.* **1988**, *7*, 123.

(5) Bouma, W. J.; Nobes, R. H.; Radom, L. *J. Am. Chem. Soc.* **1982**, *104*, 2929.

(6) Bouma, W. J.; Dawes, J. M.; Radom, L. *Org. Mass Spectrom.* **1983**, *18*, 12.

(7) Yates, B. F.; Bouma, W. J.; Radom, L. *J. Am. Chem. Soc.* **1987**, *109*, 2250.

(8) Bouma, W. J.; Nobes, R. H.; Radom, L. *J. Am. Chem. Soc.* **1983**, *105*, 1743.

(9) Postma, R.; Ruttink, P. J. A.; van Baar, B.; Terlouw, J. K.; Holmes, J. L.; Burgers, P. C. *Chem. Phys. Lett.* **1986**, *123*, 409.

(10) Yates, B. F.; Radom, L. *Org. Mass Spectrom.* **1987**, *22*, 430.

(11) Terlouw, J. K.; Heerma, W.; Dijkstra, G. *Org. Mass Spectrom.* **1981**, *16*, 326.

(12) Holmes, J. L.; Lossing, F. P.; Terlouw, J. K.; Burgers, P. C. *J. Am. Chem. Soc.* **1982**, *104*, 2930.

(13) Holmes, J. L.; Mommers, A. A.; Terlouw, J. K.; Hop, C. E. *Int. J. Mass Spectrom. Ion Processes* **1986**, *68*, 249.

(14) Stirk, K. M.; Kiminkinen, L. K. M.; Kenttamaa, H. I. *Chem. Rev.* **1992**, *92*, 1649.

(15) Mourgues, P.; Audier, H. E.; Leblanc, D.; Hammerum, S. *Org. Mass Spectrom.* **1993**, *26*, 1098.

(16) Audier, H. E.; Leblanc, D.; Mourgues, P.; McMahon, T. B.; Hammerum, S. *J. Chem. Soc., Chem. Commun.* **1994**, 2330.

(17) Audier, H. E.; Leblanc, D.; Mourgues, P.; McMahon, T. B. Poster presented at the 13th International Mass Spectrometry Conference, Budapest, Sept. **1994**.

(18) Busch, K. L.; Nixon, W. B.; Bursey, M. M. *J. Am. Chem. Soc.* **1978**, *100*, 1621.

(19) (a) Wittneben, D.; Grützmacher, H. F. *Int. J. Mass Spectrom. Ion Processes* **1990**, *100*, 545. (b) Wittneben, D.; Grützmacher, H. F. *Org. Mass Spectrom.* **1992**, *27*, 533.

(20) Audier, H. E.; Mourgues, P.; Leblanc, D.; Hammerum, S. *C. R. Acad. Sci., Ser. II* **1993**, 27.

(21) Mourgues, P.; Audier, H. E.; Hammerum, S. *Rapid Commun. Mass Spectrom.* **1994**, *8*, 53.

(22) Bjornholm, T.; Hammerum, S.; Kuck, D. *J. Am. Chem. Soc.* **1988**, *110*, 3862.

(23) Audier, H. E.; Sozzi, G.; Milliet, A.; Hammerum, S. *Org. Mass Spectrom.* **1990**, *25*, 368.

(24) Milliet, A.; LeCarpentier, E.; Audier, H. E. *Org. Mass Spectrom.* **1994**, *29*, 90.

(25) McAdoo, D. J.; Ahmed, M. S.; Hudson, C. E. *Int. J. Mass Spectrom. Ion Processes* **1990**, *100*, 579.

(26) McAdoo, D. J.; Hudson, C. E.; Sadagopa Ramanujam, V. M.; George, M. *Org. Mass Spectrom.* **1993**, *28*, 1210.

(27) Johnstone, R. A. W.; Rose, M. E. *Tetrahedron* **1979**, *35*, 2169.

(28) Milliet, A.; Sozzi, G.; Audier, H. E. *Org. Mass Spectrom.* **1992**, *27*, 787.

(29) Cooks, R. G.; Beynon, J. H.; Caprioli, R. M.; Lester, G. R. *Metastable Ions*; Elsevier: Amsterdam, 1973.

(30) Dupuis, M.; et al. *HONDO-8.1 from MOTECC 90*; IBM Corp.: Yorktown Heights, NY, 12401, 1990.

(31) Frisch, M. J.; Trucks, G. W.; Head-Gordon, M.; Gill, P. M. W.; Wong, M. W.; Foresman, J. B.; Johnson, B. G.; Schlegel, H. B.; Robb, M. A.; Replogle, F. S.; Gomperts, R.; Andres, J. L.; Raghavachari, K.; Binkley, J. S.; Gonzalez, C.; Martin, R. L.; Fox, D. J.; Defrees, D. J.; Baker, J.; Stewart, J. J. P.; Pople, J. A. *Gaussian 92*, Revision C; Gaussian, Inc.: Pittsburgh, PA, 1992.

(32) Hehre, W. J.; Radom, L.; Schleyer, P. v. R.; Pople, J. A. *Ab Initio Molecular Orbital Theory*; Wiley: New York, 1986.

(33) Pople, J. A.; Schlegel, H. B.; Krishnan, R.; Defrees, D.; Binkley, J. S.; Frisch, M. J.; Whiteside, R. A.; Hout, R. F., Jr.; Hehre, W. J. *Int. J. Quantum Chem. Symp.* **1981**, *15*, 269.

(34) McAdoo, D. J.; Hudson, C. E. *Org. Mass Spectrom.* **1986**, *21*, 779.

(35) In order to simplify Schemes 7 and 8, only one of the two pathways represented in Scheme 5 has been drawn. For the same reason, the pathways for $CH_2-CH_2^{\bullet}$ group permutation (Scheme 6) in **1b′** and **1c′** have not been drawn.

(36) Nobes, R. H.; Rodwell, W. R.; Bouma, W. J.; Radom, L. *J. Am. Chem. Soc.* **1981**, *103*, 1913.

(37) Nicolaides, A.; Borden, W. T. *J. Am. Chem. Soc.* **1991**, *113*, 6750.

(38) Lias, S. G.; Bartmess, J. E.; Liebman, J. F.; Holmes, J. L.; Levin, R. D.; Mallard, W. G. *J. Phys. Chem. Ref. Data* **1988**, *17*, Suppl. 1.

(39) However, the occurrence of a secondary isotope effect for $C_2H_4^{\bullet+}$/$C_2D_4^{\bullet+}$ transfer would give the same results, but this hypothesis becomes less likely if we also examine the unimolecular fragmentation of **1e** (Table 1). Compared with **1f** and **1g**, it gives a higher ratio of the fragment originating from structure **1e′**, which can be explained as above by the reversibility of the 1,5 migrations disturbed by the primary isotope effect.

JP9505340